The 9th European Congress on Computational Methods in Applied Sciences and Engineering
ECCOMAS Congress 2024
3–7 June 2024, Lisboa, Portugal

AN OPEN-SOURCE PHASE FIELD MODEL FOR FRACTURE IN ORTHOTROPIC FGM WITH ADAPTIVE MESH REFINEMENT

P.C.SIDHARTH[1] AND B.N.RAO[1]

[1] Department of Civil Engineering
Indian Institute of Technology Madras (IITM)
Chennai, Tamilnadu, 600036, India
e-mail: sidharthpccalicut@gmail.com

Key words: Adaptive mesh refinement, fracture, Functionally graded material, Phase-field, MOOSE

Summary. Fracture prediction in Orthotropic Functionally Graded Materials (FGM) poses a formidable challenge due to the intricate interplay of spatially varying material properties. Orthotropic FGMs, characterized by distinct material behaviors along different axes, introduce heightened complexity in modeling, particularly when addressing fracture phenomena [1]. The need for accurate and computationally efficient fracture models becomes crucial for understanding and predicting the structural response of such materials. In this context, phase field modeling emerges as a highly feasible approach, offering an effective means to simulate crack initiation, propagation, and their intricate interactions in a numerically stable manner. This paper details implementing a phase field model for fracture prediction in Orthotropic Functionally Graded Materials (FGM) within the Multiphysics Object-Oriented Simulation Environment (MOOSE), an open-source finite element framework [2]. Leveraging MOOSE's flexibility, the study incorporates a hybrid split of strain energy proposed by Ambati and introduces an adaptive mesh refinement scheme to enhance computational efficiency. The primary emphasis is on the meticulous implementation aspects, showcasing how MOOSE accommodates the complexities of orthotropic materials. Through reproducing crack paths from literature using in-house codes, the implemented model's reliability is demonstrated, validating its accuracy. The innovative use of adaptive mesh refinement not only reduces computational costs significantly but also highlights the efficiency gains achieved in simulating fracture in orthotropic FGMs. The paper underscores the advantages of utilizing MOOSE as an open-source finite element framework for transparency, collaboration, and accessibility within the research community, showcasing its role in advancing accurate and efficient fracture predictions.

1 INTRODUCTION

Functionally Graded Materials (FGMs) are advanced engineered materials characterized by a gradual variation in composition and properties, introduced by Japanese researchers in the 1980s to overcome the limitations of traditional homogeneous materials. This graded structure allows for a tailored distribution of mechanical, thermal, and electrical properties, optimizing performance in specific applications by reducing stress concentrations and enhancing structural integrity. FGMs are used across various industries, including aerospace, biomedical, and en-

ergy sectors, with fabrication methods like powder metallurgy, sol-gel processes, and additive manufacturing offering unique advantages. Their use in biomedical implants, particularly in orthopedic applications, is notable for mimicking bone properties. However, FGMs present challenges in fracture behavior, particularly when anisotropy is introduced through manufacturing processes. The phase-field modeling (PFM) approach has emerged as a powerful tool for simulating fracture phenomena in FGMs, addressing the complexities of anisotropic fracture behavior. Recent advancements in PFM, including the use of exponential finite element (EFE) shape functions, have improved computational efficiency and accuracy in modeling crack propagation in FGMs. This paper explores these advancements, comparing numerical simulations with experimental data to enhance the application of FGMs in engineering.

2 FUNCTIONALLY GRADED MATERIAL (FGM) PLATES

This study focuses on two-dimensional FGM plates with property gradation along the plate's length. The Voigt rule of mixtures is applied to homogenize the graded properties across the FGM plate, with property variations given by:

$$P(x) = P_1 + (P_2 - P_1)V_{x/y} \tag{1}$$

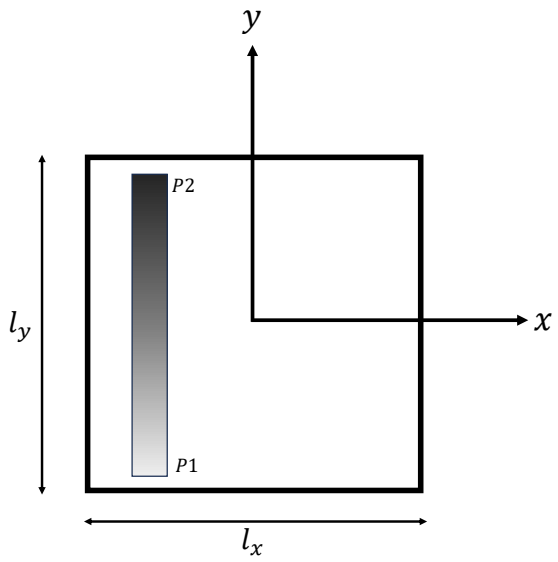

Figure 1: Model geometry and coordinate system used in Equation 1.

Here, P denotes a material property such as Young's modulus (E), Poisson's ratio (ν), or the critical energy release rate (G_c). $V_{x/y}$ is the volume fraction of the initial constituent, with gradation directions defined by:

$$V_x = \left(\frac{1}{2} - \frac{x}{l_x}\right)^p, \quad V_y = \left(\frac{1}{2} - \frac{y}{l_y}\right)^p \tag{2}$$

2.1 Orthotropic Functionally Graded Materials

Orthotropic materials display distinct mechanical properties along three mutually perpendicular axes, making them suitable for high-performance structures in aerospace, automotive, and civil engineering applications. Understanding their fracture mechanics is crucial for ensuring structural integrity.

3 PHASE-FIELD FRACTURE MODEL FOR ORTHOTROPIC FGMs

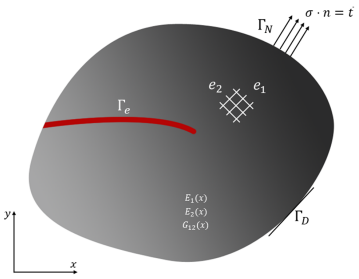

Figure 2: Schematic representation of an orthotropic FGM domain with a geometric discontinuity in the PFM framework.

In phase-field models, cracks are represented by a phase-field parameter, which transitions from 0 (intact) to 1 (cracked). The total energy, Π, in an isotropic system is:

$$\Pi = \int_\Omega \psi(\varepsilon)\,\mathrm{dV} + \int_\Omega G_c \gamma(\phi, \nabla\phi)\,\mathrm{dV} \tag{3}$$

Here, G_c is the critical energy release rate, ψ is the bulk energy, and ϕ is the phase-field order parameter. The crack surface regularization, based on Bourdin's variational formulation, is expressed as:

$$\gamma(\phi, \nabla\phi) = G_c \left(\frac{1}{2\ell}\phi^2 + \frac{\ell}{2}|\nabla\phi|^2 \right) \tag{4}$$

The bulk strain energy, incorporating a degradation term for stiffness reduction, is:

$$\Pi_b = \int_\Omega [(1-\phi)^2 + \eta]\psi_0(\varepsilon(\mathbf{u})) \tag{5}$$

$$\psi_0 = \frac{1}{2}\varepsilon^T \mathbf{C} \varepsilon \tag{6}$$

For orthotropic FGMs, the Cauchy stress tensor σ is defined as:

$$\sigma = [(1-\phi)^2 + k_p] D(x,\theta)\varepsilon \tag{7}$$

where k_p ensures numerical stability, and $D(x,\theta)$ incorporates material orientation. The linear system is then solved using the Bubnov-Galerkin method, resulting in:

$$\mathbf{K}_{uu}u^h = \mathbf{f}^{uu}, \quad \mathbf{K}_{\phi\phi}\phi^h = \mathbf{f}^{\phi} \tag{8}$$

This study considers a linearly elastic solid with spatially varying toughness $G_c(x)$ undergoing small strains. The strong form of the governing equations, without inertia forces, is described by the following system:

$$\begin{aligned} \nabla^e \cdot \sigma &= 0 \quad \text{in} \quad \Omega, \\ -G_c(x)\ell\nabla\phi\mathbf{A}\nabla\phi + \left[\frac{G_c(x)}{\ell} + 2H^+\right]\phi &= 2H^+ \quad \text{in} \quad \Gamma, \end{aligned} \tag{9}$$

where $\mathbf{A} = \mathbf{I} + \beta\left[\mathbf{I} - \mathbf{n}\otimes\mathbf{n}\right]$ accounts for crack orientation based on material orientation. Here, $\mathbf{n} = \{\cos\theta, \sin\theta\}^T$, and β serves as a penalty factor, with $\beta = 20$ used to constrain crack propagation perpendicular to the cleavage plane.

The Cauchy stress tensor for an orthotropic functionally graded material is given by:

$$\sigma = \left[(1-\phi)^2 + k_p\right] D(x,\theta)\varepsilon, \tag{10}$$

where k_p is a small positive number introduced for numerical stability. The material stiffness matrix $D(x,\theta)$ is derived as:

$$D(x,\theta) = \mathbf{T}^T\mathbf{Q}(x)\mathbf{T}, \tag{11}$$

with the transformation matrix $\mathbf{T}$ and tensor $\mathbf{Q}(x)$ defined as:

$$\mathbf{T} = \begin{bmatrix} c^2 & s^2 & 2cs \\ s^2 & c^2 & -2cs \\ -cs & cs & c^2 - s^2 \end{bmatrix}, \tag{12}$$

and

$$\mathbf{Q}(x) = \begin{bmatrix} Q_{11} & Q_{12} & 0 \\ Q_{21} & Q_{22} & 0 \\ 0 & 0 & Q_{66} \end{bmatrix}, \tag{13}$$

where the components of $\mathbf{Q}(x)$ are computed as:

$$\begin{aligned} Q_{11} &= \frac{E_1(x)}{1-\nu_{12}\nu_{21}}, \\ Q_{22} &= \frac{E_2(x)}{1-\nu_{12}\nu_{21}}, \\ Q_{12} &= \frac{\nu_{12}E_2(x)}{1-\nu_{12}\nu_{21}} = \frac{\nu_{21}E_1(x)}{1-\nu_{12}\nu_{21}}, \\ Q_{66} &= G_{12}(x), \\ \nu_{21} &= \frac{E_2(x)}{E_1(x)}\nu_{12}. \end{aligned} \tag{14}$$

The system of linear equations is then derived using the standard Bubnov-Galerkin method:

$$\begin{aligned} \mathbf{K}_{uu} u^h &= \mathbf{f}^{uu}, \\ \mathbf{K}_{\phi\phi} \phi^h &= \mathbf{f}^{\phi}, \end{aligned} \tag{15}$$

where

$$\begin{aligned} \mathbf{K}_{uu} &= \Sigma \int_{\Omega} \left[(1-\phi)^2 + k_p \right] \mathbf{B}^T \mathbf{D}(x) \mathbf{B} \, \mathrm{d}\Omega, \\ \mathbf{K}_{\phi\phi} &= \int_{\Omega} \left\{ \left[2H^+ + \frac{G_c(x)}{\ell} \right] \mathbf{N}^T \mathbf{N} + G_c(x) \ell \mathbf{B}_{\phi}^T \mathbf{B}_{\phi} \right\} \mathrm{d}\Omega, \\ \mathbf{f}^{uu} &= \Sigma \int_{\Omega} \mathbf{N}^T \bar{t} \, \mathrm{d}\Omega, \\ \mathbf{f}^{\phi} &= \Sigma \int_{\Omega} \mathbf{N}^T 2H^+ \, \mathrm{d}\Omega. \end{aligned} \tag{16}$$

4 FINITE ELEMENT IMPLEMENTATION

The domain is divided into 4-noded quadrilateral elements as part of a discretization strategy used in the finite element method to solve the phase-field fracture issue. Weak versions of the equations are obtained from this division, leading to the following construction of residual and stiffness matrices.

4.1 Discretization scheme

The domain is partitioned into 4-noded quadrilateral elements for the purpose of applying the finite element technique to phase-field fracture issues. Stiffness and residual matrices are obtained from the weak versions of the equations. Standard linear finite element (LFE) shape functions are utilized to approximate displacement, and exponential finite element (EFE) shape functions are employed to approximate the phase-field parameter. The Newton-Raphson technique is used to solve the nonlinear equations iteratively. The coupled equations are solved using Idaho National Laboratories' state-of-the-art, open-source MOOSE finite element framework. For increased efficiency and accuracy, MOOSE makes use of the Jacobian-Free Newton-Krylov (JFNK) solver. It also supports a number of physics modules for intricate simulations, such as phase-field modeling and fracture analysis. The solution is obtained through a staggered approach, calculating displacement and phase degrees of freedom alternately in load increments. The solution is obtained through a staggered approach, calculating displacement and phase degrees of freedom alternately in load increments.

4.2 Exponential finite element shape functions

Kuhn and Müller [3] gave the 1D analytical solution for a homogeneous bar exposed to tension, which was found by solving the coupled equations in (16). The phase-field variable ϕ may be expressed as follows:

$$\exp\left(\frac{-|x|}{\ell}\right) \tag{17}$$

The exponential nature of the analytical solution serves as an inspiration for the creation of exponential finite element (EFE) shape functions. To properly capture this exponential behavior, the authors recommended using EFE shape functions rather than more conventional linear finite element (LFE) form functions. The 1D exponential finite element (EFE) shape functions are given by: $\xi' \in [-1, 1]$, which is a function of the natural coordinate in 1D.

$$\bar{N}_1^e(\xi', \delta) = 1 - \frac{\exp\left(-\frac{\delta(1+\xi')}{4}\right) - 1}{\exp\left(-\frac{\delta}{2}\right) - 1} \quad \bar{N}_2^e(\xi', \delta) = \frac{\exp\left(-\frac{\delta(1+\xi')}{4}\right) - 1}{\exp\left(-\frac{\delta}{2}\right) - 1} \tag{18}$$

Unlike linear finite element (LFE) shape functions, which are symmetric and independent of ϕ, proper orientation of EFE form functions with respect to nodal phase-field values is critical to accuracy. See [4] for further information on the orientation scheme, derivatives of EFE shape functions, and their two-dimensional representation.

4.3 Automatic orientation of EFE shape functions

The asymmetry of exponential finite element (EFE) shape functions requires alignment with the evolving crack path, which is unknown until a critical load increment is reached. The study uses an automatic orientation scheme that starts with linear finite element (LFE) shape functions. Elements are marked for correction with EFE shape functions based on the sum of the phase-field variable at their nodes. The orientation of EFE shape functions is then determined for these elements, and the analysis is restarted from a lower load increment.

5 NUMERICAL EXAMPLES AND DISCUSSION

5.1 Single Edge Notched Orthotropic Rectangular FGM Plate (SEN-FGM)

Traditional fracture analysis has mainly focused on homogeneous orthotropic materials. With the introduction of functionally graded materials (FGMs), new challenges and opportunities have emerged. FGMs exhibit a gradual variation in properties, which enhances their ability to withstand thermal and mechanical stresses. This study investigates the fracture behavior of orthotropic FGM plates, focusing on unique crack propagation mechanisms due to material gradients. The study simplifies the complex variation of material properties by assuming an exponential gradation:

$$\begin{aligned} E_1(x) &= E_1 \cdot e^{\alpha x} \\ E_2(x) &= E_2 \cdot e^{\beta x} \\ G_{12}(x) &= G_{12} \cdot e^{\gamma x} \end{aligned} \tag{19}$$

Material properties vary proportionally with indices set to 0.2. The finite element mesh includes approximately 24,000 elements with selective refinement where cracks are anticipated. The chosen length scale parameter is 0.0015 mm, and an average mesh size of over 0.003 mm ensures the applicability of EFE shape functions [3].

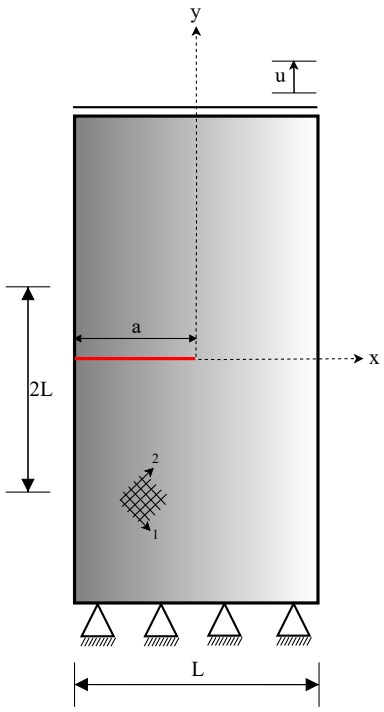

Figure 3: Geometry and boundary conditions of SEN-FGM specimen 5.1 showing functionally graded properties along x-axis

Property	Value
Longitudinal stiffness E_{11}	114.8 GPa
Transverse stiffness E_{22}, E_{33}	11.7 GPa
Shear stiffness G_{12}	9.66 GPa
Major Poisson's ratio ν_{12}	0.21
Critical energy release rate G_f	2.7 N/mm

Table 1: Material properties of SEN-FGM specimen (5.1)

5.1.1 Direction of FGM Gradation

The gradation direction significantly influences crack nucleation and propagation. Examining the plate with a crack perpendicular to the gradation direction (Y-direction), we find that crack propagation paths are similar regardless of whether gradation is along the X or Y direction. However, Figure 5 shows that load responses differ, with increased stiffness for X-direction gradation compared to Y-direction.

5.1.2 Orientation of the Orthotropic Material Axis

This study assesses the effectiveness of EFE shape functions for predicting fractures in orthotropic FGMs. Crack paths for various material axis orientations (30°, 45°, and 60°) are

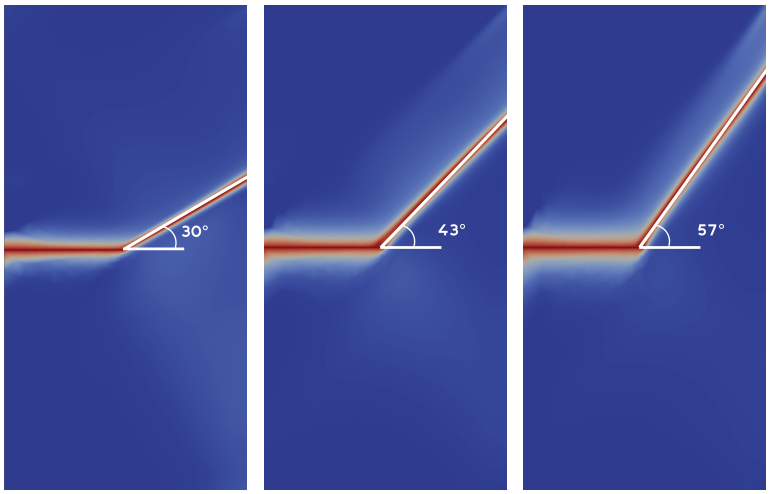

(a) (b) (c)

Figure 4: Crack trajectory predicted by EFE shape functions for SEN-FGM specimen: (a) θ=30°, (b) θ=45°, (c) θ=60°

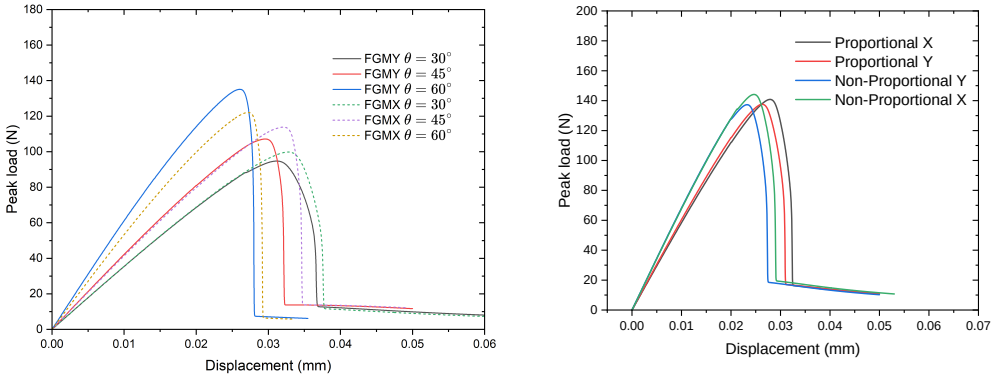

(a) (b)

Figure 5: (a) Comparison of load-displacement response for the orthotropic FGM sample with different material orientations; gradation of FGM properties in X and Y directions. (b) Comparison of load-displacement response for the orthotropic material with different material orientations, SEN-FGM sample.

compared with experimental data from Cahill et al. [5]. Table 2 compares crack propagation angles with experimental and phase-field model results.

5.1.3 Gradation of FGM Properties

The impact of material property gradation on fracture responses is examined. Two types of exponential gradation are considered: proportional (with α, β, and γ set to 0.2) and non-

Orientation of fibres (θ)	30°	45°	60°
Cahill et al. (Experimental [5])	30	45	60
Hirshikesh et al. (Phase-field [**?**])	29.1	43	55
Present study (EFE-Phase-field)	30	43	57

Table 2: Comparison of crack propagation angles with experimental data and phase-field models, SEN-FGM specimen

proportional (with α=0.5, β=0.4, and γ=0.3). The material properties remain consistent with previous parameters. Force-displacement responses indicate that non-proportional grading yields stiffer responses compared to proportional grading, with slight increases in peak load for X-direction gradation.

6 CONCLUSIONS

In this study, the use of Exponential Finite Element (EFE) shape functions to assess the mechanical response of an orthotropic functionally graded plate has provided significant insights. By examining benchmark examples, various factors affecting crack propagation were explored, including the orientation of material orthotropy, the direction of FGM gradation, and the type of gradation. The EFE shape functions effectively predicted crack propagation paths in alignment with material directions, demonstrating their capability to capture the complex behavior of orthotropic functionally graded materials (FGMs).

REFERENCES

[1] Hirshikesh and Martínez-Pañeda, Emilio and Natarajan, Sundararajan, *Defence Technology*, Vol. **17**, pp. 185–195, 2021.

[2] D. Schwen and L.K. Aagesen and J.W. Peterson and M.R. Tonks, Rapid multiphase-field model development using a modular free energy based approach with automatic differentiation in MOOSE/MARMOT *Computational Materials Science*, Vol. **132**, pp. 36-45, 2017.

[3] C. Kuhn, R. Müller, Journal of Theoretical and Applied Mechanics **49** (2011). http://www.ptmts.org.pl/jtam/index.php/jtam/article/view/v49n4p1115/227

[4] P.C. Sidharth, B.N. Rao, Engineering Fracture Mechanics **291**, 109576 (2023). https://doi.org/10.1016/j.engfracmech.2023.109576

[5] L.M.A. Cahill, S. Natarajan, S.P.A. Bordas, R.M. O'Higgins, C.T. McCarthy, Compos. Struct. **107**, 119 (2014). https://doi.org/10.1016/j.compstruct.2013.05.039